Phase separation and microstructure evolution of rapidly quenched Gd–Hf–Co–Al alloys

J.H. Han [a,b,*], N. Mattern [a], D.H. Kim [c], J. Eckert [a,b]

[a] *IFW Dresden, Institute for Complex Materials, Helmholtzstr. 20, 01069 Dresden, Germany*
[b] *TU Dresden, Institute of Materials Science, Helmholtzstr. 7, 01069 Dresden, Germany*
[c] *Center for Non-Crystalline Materials, Yonsei University, 134 Shinchon-dong, Seodaemun-gu, Seoul 120-749, South Korea*

ARTICLE INFO

ABSTRACT

Phase separated metallic glasses were prepared in the Gd–Hf–Co–Al system by rapid quenching of the melt. Due to the strong positive enthalpy of mixing between the main constituent elements Gd and Hf (ΔH_{Gd-Hf} = +11 kJ/mol) a heterogeneous microstructure is formed consisting of two amorphous phases, which are Gd-enriched and Hf-enriched, respectively. The size of the phase separated regions varies from 0.1 μm to 5 μm, depending on alloy composition and cooling rate. Different types of microstructure, such as an interconnected structure or a droplet structure were obtained as a function of cooling rate. The microstructure of the phase separated metallic glasses is determined not only by their composition, the critical temperature, and the shape of the miscibility gap, but also by the viscosity and diffusivity of the melt.

1. Introduction

Since the first finding of liquid state phase separation in the La–Zr–Al–Ni–Cu system [1], the strategy to develop in situ glass–glass composites containing two compositionally different amorphous phases, were successfully developed in different alloy systems. Examples for such systems are Ti–Y–Co–Al [2], Ni–Nb–Y [3], Cu–Zr–Al–Y [4] and Gd–Ti–Co–Al [5]. These systems consist of element combinations with high glass-forming ability (GFA) on one hand, and a strong positive enthalpy of mixing between certain constituent elements (i.e. ΔH_{Nb-Y} = +30 kJ/mol, ΔH_{Ti-Y} = +15 kJ/mol, ΔH_{Zr-Y} = +35 kJ/mol and ΔH_{Gd-Ti} = +15 kJ/mol) [2–5] on the other hand. The requirement of adding an element with a positive enthalpy of mixing to any of the components of the alloy usually reduces the glass-forming ability and, therefore, rapid quenching of the melt is necessary in order to prepare a phase separated metallic glass. As well as in nano-structured and other conventional crystalline materials, the microstructure evolution affects the properties of phase separated metallic glassy alloys [6,7]. The characteristic types of microstructure of phase separated metallic glasses can be classified into a droplet-like or an interconnected structure, which develop by nucleation and growth or by spinodal decomposition, respectively [8]. An improvement of mechanical properties was found for some phase separated metallic glasses, which was attributed to the heterogeneities hindering the movement of shear bands [9,10]. Moreover, the phase separated structure has received attention as a useful way to fabricate porous metallic glassy material by selective dissolution of one of the constituent phases [11,12].

In this paper, we report on the composition and cooling rate dependence of the microstructure evolution in rapidly quenched $Gd_{55-x}Hf_xCo_{25}Al_{20}$ (x = 10, 20, 27.5, 35, 45 and 55 at.%) metallic glasses. The alloy compositions were chosen because they fulfil the prepositions to prepare phase separated metallic glasses. The ternary $Gd_{55}Co_{25}Al_{20}$ and $Hf_{55}Co_{25}Al_{20}$ alloys exhibit a rather high glass-forming ability and monolithic bulk glassy specimens of ~2 mm in diameter have been successfully produced [13–15]. Due to the large positive enthalpy of mixing between Gd and Hf (ΔH_{Gd-Hf} = +11 kJ/mol), decomposition of Gd–Hf–Co–Al melts into Gd-rich and Hf-rich phases during quenching is expected. We will show that besides the chemical composition also the cooling rate determines the morphology of the microstructure with respect to formation of a droplet-type or an interconnected-type structure.

2. Experimental

Pre-alloyed ingots of $Gd_{55-x}Hf_xCo_{25}Al_{20}$ (x = 0, 10, 20, 27.5, 35, 45, 55) were prepared by arc-melting in an argon atmosphere starting from elements with a purity of 99.9% or higher. To achieve homogeneity, the ingots were remelted 3 times and cast into a water-cooled Cu mold of cylindrical rod-shape with 5 mm diameter by suction casting. From these rod-shape pre-alloys, ribbon samples with 3–4 mm in width and 25–30 μm in thickness were fabricated by single-roller melt spinning

* Corresponding author at: IFW Dresden, Institute for Complex Materials, Helmholtzstr. 20, 01069 Dresden, Germany. Tel.: +49 351 4659 813; fax: +49 351 4659 452.

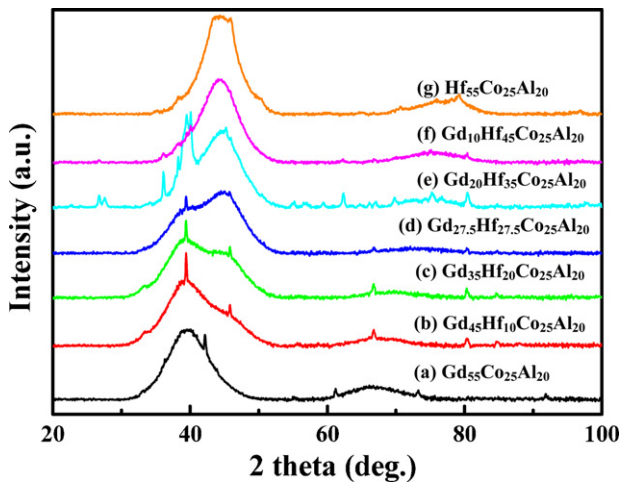*E-mail address:* j.han@ifw-dresden.de (J.H. Han).

Fig. 1. XRD patterns of rapidly quenched $Gd_{55-x}Hf_xCo_{25}Al_{20}$ alloys ($x = 0$, 10, 20, 27.5, 35, 45 and 55).
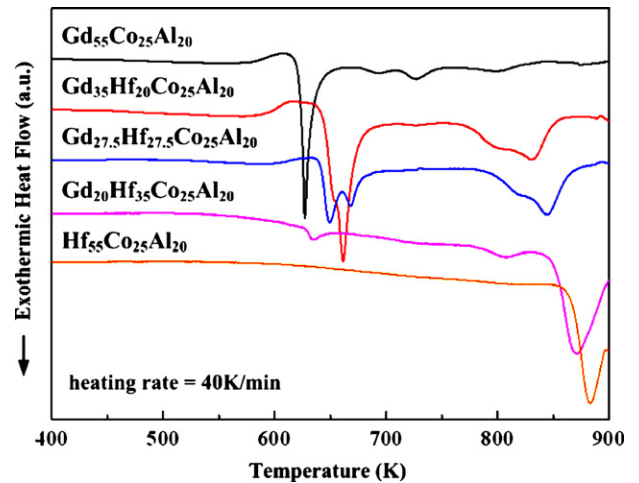

Fig. 2. DSC traces obtained for rapidly quenched $Gd_{55}Co_{25}Al_{20}$, $Hf_{55}Co_{25}Al_{20}$, $Gd_{35}Hf_{20}Co_25Al_{20}$, $Gd_{27.5}Hf_{27.5}Co_{25}Al_{20}$ and $Gd_{20}Hf_{35}Co_{25}Al_{20}$ ribbons with a heating rate 40 K/min. The exothermic peaks in the low temperature range correspond to crystallization of the Gd-rich amorphous phase, and the peaks at the high temperature range to that of the Hf-rich amorphous phase, respectively.

with quartz crucible in an argon atmosphere. The wheel speed and the casting temperature measured with a pyrometer were 30 m/s and 1600–1700 K, respectively. The structures of the ribbon samples were analysed by X-ray diffraction (XRD) with Co Kα radiation (Panalytical X'Pert Pro). To investigate the thermal stability, differential scanning calorimeter (Perkin Elmer DSC7) with a heating rate of 40 K/min was performed. A scanning electron microscope (SEM) (Gemini–Zeiss) equipped with an energy-dispersive spectrometer (EDX) was applied for microstructure observation and quantitative analysis of chemical compositions.

3. Results and discussion

The XRD patterns of as-quenched $Gd_{55-x}Hf_xCo_{25}Al_{20}$ ($x = 0$, 10, 20, 27.5, 35, 45 and 55) ribbons are shown in Fig. 1. The broad diffuse patterns indicate that these as-quenched ribbons are mainly amorphous phase (Fig. 1(a)–(g)). Sharp diffraction peaks indicate that also some crystalline phases such as Gd_2Co_2Al are present for all alloys [16]. The unusual diffraction pattern for alloy with $x = 55$ at.%

Hf in Fig. 1(g) is indicating superposition of amorphous matrix and cF96 Hf_2Co phase [15]. The appearance of two diffuse maxima for $x = 10$–45 at.% in Fig. 1(b)–(f) gives evidence for phase separation in these glasses. The first maximum around diffraction angles ($2\theta \approx 39.8°$) corresponds to a Gd-rich phase and that at higher diffraction angles ($2\theta \approx 44.2°$) to an Hf-rich phase, respectively. With increasing Hf-content, the intensity of the second diffuse maximum becomes larger and that of the first maximum decreases, which indicates the change in volume fraction of the respective phases with composition. From the area of the maxima determined by Gaussian fitting the volume fractions of the two amorphous phases were estimated. The obtained values are given in Table 1. Within the error limits a linear dependence is found. The two-phase glassy structure is also confirmed by DSC investigations. Fig. 2 shows the
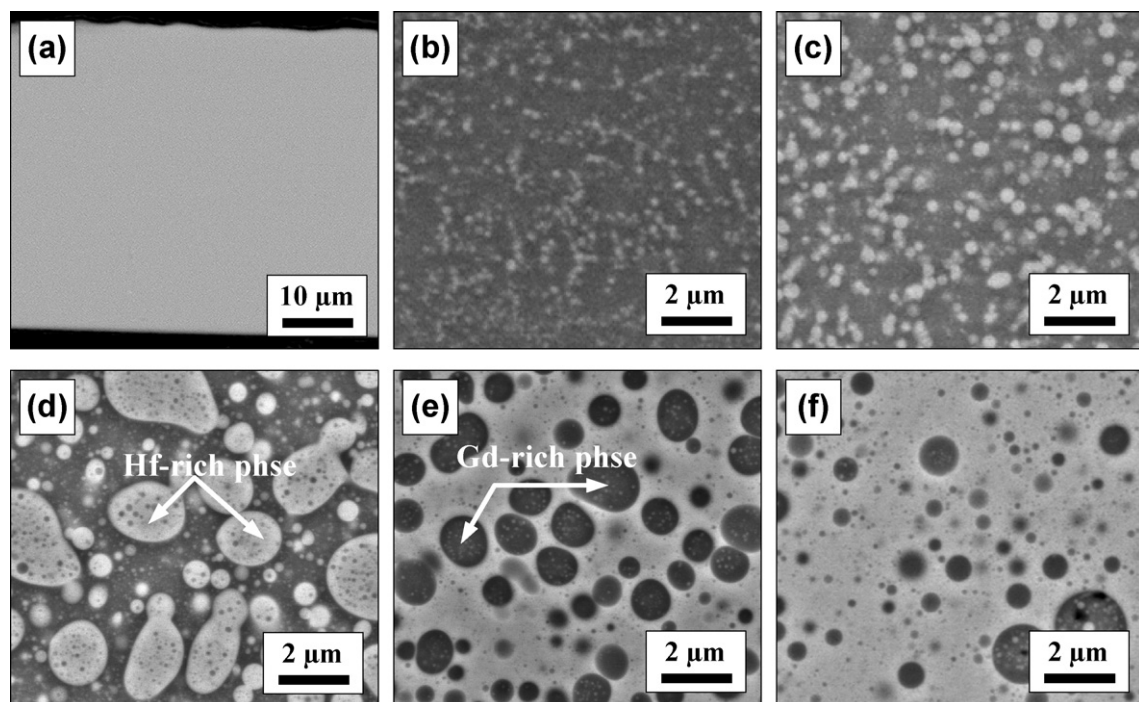

Fig. 3. Backscattered electron micrographs obtained from the cross-section of rapidly quenched (a) $Gd_{55}Co_{25}Al_{20}$, (b) $Gd_{45}Hf_{10}Co_{25}Al_{20}$, (c) $Gd_{35}Hf_{20}Co_{25}Al_{20}$, (d) $Gd_{27.5}Hf_{27.5}Co_{25}Al_{20}$, (e) $Gd_{20}Hf_{35}Co_{25}Al_{20}$ and (f) $Gd_{10}Hf_{45}Co_{25}Al_{20}$ ribbons.
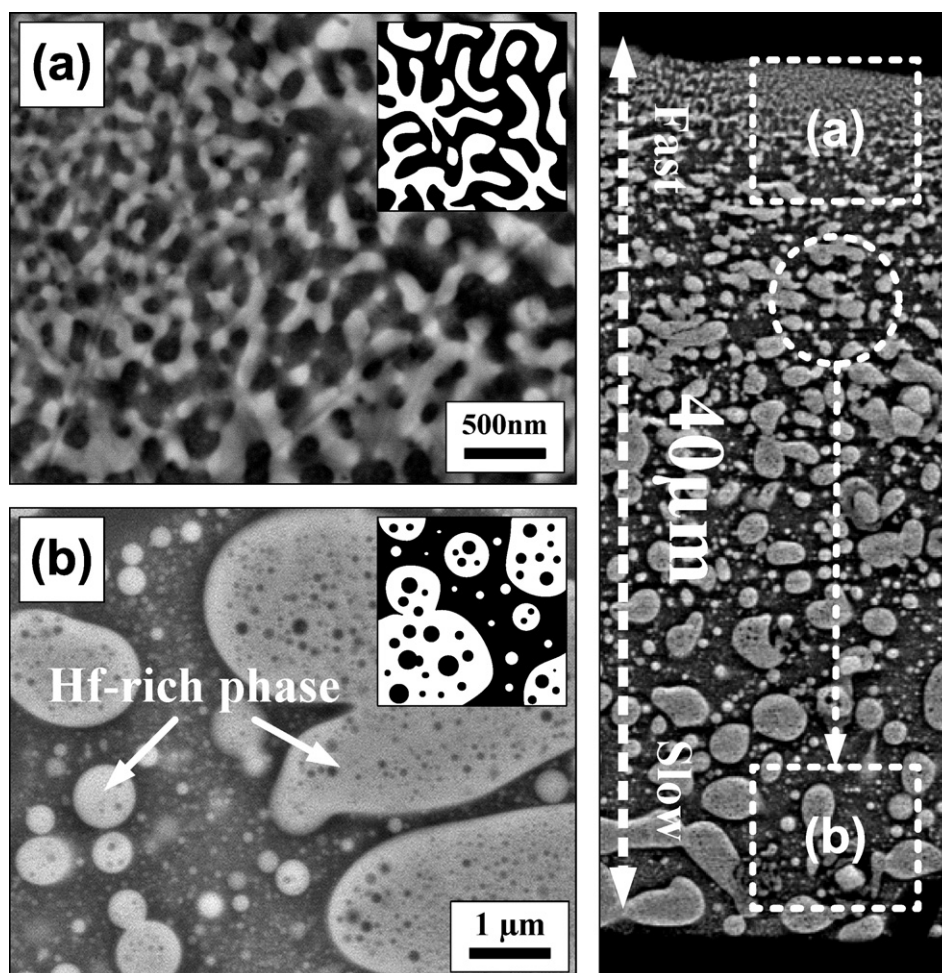
Fig. 4. (a) and (b) Backscattered electron micrographs of rapidly quenched $Gd_{27.5}Hf_{27.5}Co_{25}Al_{20}$: (a) highly magnified backscattered electron micrograph of $Gd_{27.5}Hf_{27.5}Co_{25}Al_{20}$ obtained from the wheel side of the ribbon with highest cooling rate, (b) micrograph obtained from free side of the cross-section with lower cooling rate. The overview of the cross-section is displayed on the right-hand side.

DSC traces obtained for the as-quenched $Gd_{55-x}Hf_xCo_{25}Al_{20}$ ($x = 0$, 20, 27.5, 35, 55) ribbons recorded with a heating rate of 40 K/s. The decomposed state of the Gd–Hf–Co–Al alloys is indicated by separated crystallization events at distinctly different temperatures upon heating. The two exothermic events observed for the alloys with $x = 20$, 27.5, and 35 represent the crystallization of the Gd-rich amorphous phase at lower temperature ($T_{x1} \approx 620$–650 K), and the Hf-rich amorphous phase crystallizes at higher temperature ($T_{x2} > 830$ K), respectively, as it can be inferred from comparison with single-phase Gd-rich and Hf-rich glasses [13–15]. When the Hf content increases from $x = 0$ to $x = 35$, a decrease of the heat flow of the first exothermic event corresponding to crystallization of the Gd-rich phase is observed. This related with volume fraction change of the Gd-rich phase while composition varies. The disappearance of the exothermic peak of the Gd-rich phase in the alloy with $x = 35$

can be explained by partial crystallization of the Gd-rich phase, as shown by the XRD pattern of the as-quenched ribbon.

The series of SEM micrographs depicted in Fig. 3 shows the influence of composition on the microstructure evolution and the morphology of the phase separated metallic glasses for samples with different Gd-to-Hf ratio. A heterogeneous droplet-like structure is observed for all compositions. By EDX analysis, the dark areas can be attributed to the Gd-enriched phase, and the bright areas correspond to the Hf-enriched phase, respectively. The volume fractions of the different alloys were calculated from the corresponding areas of the cross section. The obtained values given in Table 1 are in good agreement with the XRD-data. The chemical compositions of the two phases were determined by analysing several EDX area spectra (about 1 μm × 1 μm). The corresponding values are also given in Table 1. These data represent the chemical

Table 1
Volume fractions of the Gd-rich phases estimated from X-ray diffraction and SEM micrographs. Chemical compositions of the two glassy phases are determined by EDX.

Alloy composition	Vol.% Gd-rich from XRD	Vol.% Gd-rich from SEM	Gd-rich phase	Hf-rich phase
$Gd_{55}Co_{25}Al_{20}$	100	100	$Gd_{51.3}Co_{28}Al_{20.7}$	–
$Gd_{45}Hf_{10}Co_{25}Al_{20}$	77	82	–	–
$Gd_{35}Hf_{20}Co_{25}Al_{20}$	63	66	–	–
$Gd_{27.5}Hf_{27.5}Co_{25}Al_{20}$	36	45	$Gd_{35.9}Hf_{14.8}Co_{21.8}Al_{27.5}$	$Gd_{14.1}Hf_{33.8}Co_{31.5}Al_{20.6}$
$Gd_{20}Hf_{35}Co_{25}Al_{20}$	23	31	$Gd_{39}Hf_{13.3}Co_{14.7}Al_{33}$	$Gd_{11.2}Hf_{38.6}Co_{28.2}Al_{22}$
$Gd_{10}Hf_{45}Co_{25}Al_{20}$	8	15	–	$Gd_{8.4}Hf_{43.2}Co_{24.8}Al_{23.6}$
$Hf_{55}Co_{25}Al_{20}$	0	0	–	$Hf_{49.9}Co_{25.3}Al_{24.8}$

compositions of the two liquids after the first stage of decomposition. The two liquids exhibit also different Co and Al contents. Due to supersaturation during further quenching, secondary precipitates occur, which can be clearly seen within the droplets. In addition, reversion of the contrast of precipitates and matrix phase occurs in for the alloys with Hf contents 27.5–35 at.%. The microstructure observations reveal that the liquid with larger volume forms the matrix and the droplet-like domains represent the minority liquid phase for all compositions. When the Hf content increases to 27.5 at.%, the size of the spherical-shaped precipitates increases from about 100 nm, i.e. the size that can just be resolved by SEM, to about 5 μm in size. For larger Hf contents, the size drops again. The analysis of the microstructures as a function of composition reveals that the miscibility gap of the Gd–Hf–Co–Al phase separating system is asymmetric and that the maximum critical temperature of the miscibility gap should be in the range of Hf contents $27.5 < x < 35$. The distinct size difference of the droplet-like phase in both alloys with Hf contents $x = 20$ and $x = 35$, which can be seen in Fig. 3(b) and (d) is related to the temperature difference between the critical temperature (T_c) of the miscibility gap and the glass transition temperature (T_g) of each droplet-like phase.

Fig. 4 shows the two different types of microstructures found in the rapidly quenched $Gd_{27.5}Hf_{27.5}Co_{25}Al_{20}$ ribbon together with schematic drawings as insets. An overview of the ribbon cross section is displayed on the right hand side in Fig. 4. The regions where both micrographs were taken are presented by dashed squares. Regions (a) and (b) at both surface-near regions represent the influence of the cooling rate, which decreases from the wheel surface at region (a) to the free surface at region (b). A fine tortuous structure in Fig. 4(a) and a typical droplet-like structure in Fig. 4(b) are obtained for each surface subjected to different cooling rates. This difference of such domain morphology in the phase-separated metallic glass alloys can be explained by the lattice Boltzmann model [17].

The lattice Boltzmann model describes the coarsening of a phase-separated liquid. The time dependence of the microstructure development is determined by the viscosity of the liquids and the diffusivity of the elements. Simulation of the time-dependent development of domain patterns for liquids with intermediate viscosity and low diffusivity are in good agreement with our experimental observations. The microstructure found for the area close to the wheel surface (Fig. 4(a)) represents the early stage of coarsening with high connectivity. On the other hand, the typical droplet-like structure with coalescence and grown spherical shapes in Fig. 4(b) is in good agreement with the final stage. The progress of the microstructural development of the $Gd_{27.5}Hf_{27.5}Co_{25}Al_{20}$ alloy due to local variation of the cooling rate in the ribbon is indicated by the dashed circle and the arrow in the right-hand side of Fig. 4. This variation in cooling rate can be correlated with the change of the microstructure with time from the numerically calculated domain development progress, as shown in Fig. 4 in Ref. [17].

4. Conclusion

The present study shows that liquid state phase separation occurs when Hf replaces Gd in Gd–Co–Al ternary liquids and that phase separated metallic glasses can be prepared by rapid quenching of the melt. These quaternary alloys decompose into two Gd-rich and Hf-rich amorphous phases with different size and secondary phase separation. The sizes range from about 100 nm to 5 μm, respectively. The microstructural characteristics of the liquid state phase separated Gd–Hf–Co–Al alloys, such as the reversal of matrix phase and precipitated phase, and the volume fractions of each phase, are determined by the chemical composition of the alloys. In addition, the cooling rate dependence of the microstructure can be revealed by cross sectional SEM imaging. Different types of microstructures, such as an interconnected structure or a droplet structure, are observed for the fast and slowly cooled regions of the $Gd_{27.5}Hf_{27.5}Co_{25}Al_{20}$ sample, respectively. These results reveal that the microstructure of phase separated metallic glasses is determined not only by their composition, the critical temperature, and the shape of the miscibility gap but also by the viscosity and diffusivity of the melt.

Acknowledgements

References

[1] A.A. Kündig, M. Ohnuma, D.H. Ping, T. Ohkubo, K. Hono, Acta Mater. 52 (2004) 2441–2448.
[2] B.J. Park, H.J. Chang, W.T. Kim, D.H. Kim, Appl. Phys. Lett. 85 (2004) 6353–6355.
[3] N. Mattern, U. Kühn, A. Gebert, T. Gemming, M. Zinkevich, H. Wendrock, L. Schultz, Scripta Mater. 53 (2005) 271–274.
[4] E.S. Park, D.H. Kim, Acta Mater. 54 (2006) 2597–2604.
[5] H.J. Chang, W. Yook, E.S. Park, J.S. Kyeong, D.H. Kim, Acta Mater. 58 (2010) 2483–2491.
[6] C.C. Hays, C.P. Kim, W.L. Johnson, Phys. Rev. Lett. 84 (2000) 2901.
[7] U. Kühn, J. Eckert, N. Mattern, L. Schultz, Appl. Phys. Lett. 80 (2002) 2478.
[8] B.J. Park, H.J. Chang, D.H. Kim, W.T. Kim, K. Chattopadhyay, T.A. Abinandanan, S. Bhattacharyya, Phys. Rev. Lett. 96 (2006) 245503.
[9] Y.H. Liu, G. Wang, R.J. Wang, D.Q. Zhao, M.X. Pan, W.H. Wang, Science 315 (2007) 1385–1388.
[10] E.S. Park, J.S. Kyeong, D.H. Kim, Scripta Mater. 57 (2007) 49–52.
[11] A. Gebert, A. Kündig, L. Schultz, K. Hono, Scripta Mater. 51 (2004) 961–965.
[12] J. Jayaraj, B.J. Park, D.H. Kim, W.T. Kim, E. Fleury, Scripta Mater. 55 (2006) 1063–1066.
[13] D. Chen, A. Takeuchi, A. Inoue, Mater. Sci. Eng. A 457 (2007) 226–230.
[14] D. Chen, A. Takeuchi, A. Inoue, Mater. J. Mater. Sci. 42 (2007) 8662–8666.
[15] D.V. Louzguine, H. Kato, H.S. Kim, A. Inoue, J. Alloys Compd. 359 (2003) 198–201.
[16] J. Wan, Acta Metall. Sin. 30 (1993) 204.
[17] A.J. Wagner, J.M. Yeomans, Phys. Rev. Lett. 80 (1998) 1429–1432.